Doppler Sodar Analysis of Frontal Friction in Relation to Frontal Slope

B. S. GERA* AND A. WEILL

CNET/CRPE/CNRS—38/40, rue du Général Leclerc, 92131—Issy-les-Moulineaux, France

(Manuscript received 22 August 1986, in final form 7 January 1987)

ABSTRACT

Doppler sodar information on the wind field in relation to frontal slope observed on reflectivity facsimile records was considered during Mesogers 84 experiment. The data have been analyzed to examine and quantify the correlation between vertical (updraft/downdraft) velocities and the frictional velocity in the surface layer. Based on theoretical considerations, the frontal slope modifications due to divergence of frontal friction have been quantified, and the associated drag coefficients are tentatively established. It has been observed that the downdraft velocities tend to increase with the horizontal wind speed in the surface layer. Frontal slope is directly proportional to the magnitude of momentum transfer (in the direction of front propagation) caused by friction velocity in the surface layer. Estimated values of drag are realistic.

1. Introduction

Friction velocity in the atmospheric surface layer plays an important role in the numerical modeling of the planetary boundary layer (Long and Shaffer, 1975) in order to understand the relative importance of the various external and internal processes in determining the boundary layer behavior. In this context, external factors are generally related to large-scale synoptic conditions, while internal factors are associated with the vertical transport of the eddy fluxes of heat, momentum and moisture. The boundary layer quantities governing these parameters are basically the prevailing wind, temperature and pressure fields. The diurnal variations in the wind and temperature field are determined by the intervening terrain roughness and time of the day, and small-scale fluctuations which depend on atmospheric stability conditions. However, large-scale fluctuations are governed by the dynamics of mesoscale disturbances, especially the frontal systems, and are dependent on the nature of their origin (Scott and Ackerman, 1983; Johnson and Nicholls, 1983).

The terrain interactions with the wind field in the surface layer are characterized by the friction velocity U_* associated with eddy flux of vertical momentum transfer $u'w' = -U_*^2$, where u' and w' are the perturbations of longitudinal and vertical velocity, respectively. This vertical transfer of momentum is often described for mesoscale phenomena in terms of drag coefficient (Mason and Sykes, 1978). Therefore, for a better understanding of the boundary layer interactions with mesoscale disturbances, frontal friction and associated vertical velocities, momentum transfer and drag coefficients have to be studied.

Fronts are generally characterized by their slope and their propagating velocity vector and hence can be analyzed from Doppler sodar information in the lower part of the atmospheric boundary layer. Wind field information and facsimile records of reflectivity (backscattering acoustic intensity) particularly, can give some insight into dynamics of fronts. The purpose of this paper is to present an analysis of frontal slope in the lower part of the boundary layer (considering modifying factors related to divergence of the momentum transfer), and to apply the results to Doppler sodar data.

Doppler sodar data and meteorological data will be taken from the Mesogers 84 experiment, which was held in the southwest of France during the period 10 September–5 October 1984 (Weill et al., 1986), and will be used to estimate frontal slope, divergence of momentum transfer, frontal drag coefficient and to statistically evaluate properties of frontal vertical motion.

2. Theoretical considerations

a. *Frontal slope*

To derive an expression for the frontal slope, we begin with the momentum equation for an incompressible stratified shear layer obeying the Boussinesq approximations.

The atmospheric flow is assumed to be without divergence and the reference state obeys the hydrostatic equilibrium. With these assumptions, if z is the vertical coordinate, y a horizontal coordinate parallel to the direction of frontal movement and x parallel to the

* Permanent affiliation: National Physical Laboratory, New Delhi, India.

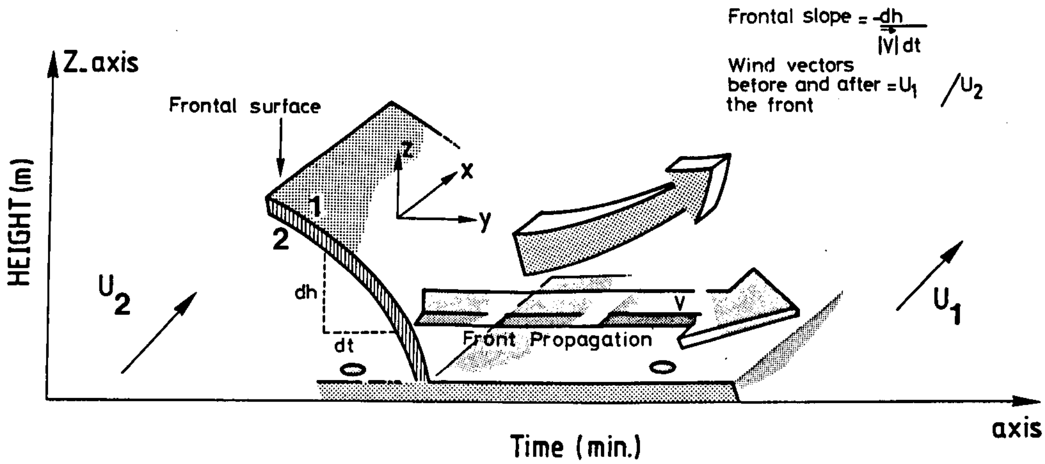

FIG. 1. Representation of front motion with respect to coordinate system: y is taken as parallel to the front propagation velocity **V**, x is taken along the frontal surface; i.e., perpendicular to y. The wind velocities are $\mathbf{U}_1$ and $\mathbf{U}_2$, respectively, before and after the front.

front (Fig. 1), the vertical gradient of momentum transfer can be written as

$$\frac{\partial\tau}{\partial z}=fu_x-\frac{1\partial P}{\rho\partial y} \tag{1}$$

where f is the Coriolis parameter, u_x the horizontal wind speed (component along x axis), P the pressure, τ the Reynolds stress $= -\rho U_*^2$, and ρ the air density.

Assuming the pressure balance $dP_{12} = 0$ across the frontal surfaces 1 and 2 (Fig. 1), we obtain

$$\frac{dz}{dy}=\left(\frac{\partial P_1}{\partial y}-\frac{\partial P_2}{\partial y}\right)\Big/(\rho_{01}-\rho_{02})g \tag{2}$$

where ρ_0 is the reference density and dz/dy is the frontal slope.

Development of (2) with the previous hypothesis and (1) gives

$$\frac{dz}{dy}\approx\frac{fT}{g}\frac{(u_{2x}-u_{1x})}{(T_1-T_2)}+\frac{T}{g(T_1-T_2)}\frac{(\partial\tau 1-\partial\tau 2)}{\partial z-\partial z}, \tag{3}$$

where u_{1x} and u_{2x} are components along x for regions 1 and 2, and T is the mean temperature. The first term at the right of (3) is what can be described as the classic slope, and the second term a correction term to account for the interaction with the boundary layer.

The classic slope is determined by the behavior of the prevailing wind and temperature fields across the frontal surface and the modifying factor depends on the temperature field and on the vertical divergence of momentum transfer in the direction of the frontal movement across the frontal surface.

Based on Eq. (3), the slope modification due to the frontal friction can be calculated using Doppler sodar information related to sodar facsimile records of reflectivity (acoustic backscattering intensity of reflectivity, proportional to C_T^2), denominated echograms and the prevailing wind field conditions, in addition to temperature measurements.

b. *Frontal drag coefficient*

Basically, the drag coefficient C_d is associated with the transfer of momentum by the relationship

$$C_d=-\tau/\rho U^2, \tag{4}$$

where U is, in general, the mean horizontal wind speed. For a frontal system propagating along the y axis with $\Delta\tau_y = |\tau_1 - \tau_2|$ and the wind difference $\Delta u_y = |u_{1y} - u_{2y}|$ along the line of propagation, the associated drag coefficient via an analogy to Eq. (4) is given by

$$\Delta\tau_y=-\rho C_{df}|\Delta u_y|^2 \tag{5}$$

where ρ and C_{df} are assumed to be mean properties of the frontal discontinuity and not to vary considerably with space along the direction of front propagation. Thus, the divergence of momentum transfer related to the front is given by

$$\frac{\partial(\tau 1-\tau 2)}{\partial z}=-\rho C_{df}\frac{\partial(\Delta uy)^2}{\partial z}. \tag{6}$$

Therefore, a knowledge of the magnitude of momentum transfer through sodar analysis of the frontal slope can be further used to estimate frontal drag coefficient.

3. Data analysis

a. *Data description*

Doppler sodar of C.R.P.E. used in this study is a monostatic system with three antennas and has been described in Weill et al. (1978). With a 2000 Hz acoustic frequency, a 100 ms pulse duration corresponding to a gates dimension of 17 m and a repetition period of 4 s (simultaneously on every antenna), it gives information on the horizontal wind field which has been averaged over a 20 min period from 20 m up to 550 m height. Following section 2a, we shall estimate frontal slope (using facsimile records of reflectivity on the three antennas of the sodar system), frontal propagation velocity and wind components in the direction parallel and perpendicular to the frontal motion, as shown in Fig. 1.

b. Methodology

The basic approach for the present analysis lies in estimating the real frontal slope near the surface from facsimile records and estimating wind components u_{1x} and u_{2x}. Figure 1 shows that the vertical antenna of sodar maps the frontal height dh in dt seconds. If the front propagation velocity $\mathbf{V}$ near the surface is known, the frontal slope can be computed through the relation

$$\frac{dz}{dy} = \left| -\frac{dh}{Vdt} \right| \quad (7)$$

where $V = |\mathbf{V}|$.

Wind components u_1 and u_2 require knowledge of frontal movement relative to the sodar system. The three-antenna system is positioned in Fig. 2a: antenna 3 points vertically, and antennas 1 and 2 are slanting at thirty degrees from vertical antenna axis. The three-sample volume defines the vertices of an isosceles triangle, from which frontal velocity can be computed. A frontal system passing over the vertical antenna (Fig. 2b) at an altitude dh will travel a horizontal distance $d_1 = d/V\cos\theta$ before being observed through sodar 1, and a distance $d_2 = d/\cos(\pi/2 - \theta)$ before detection by sodar 2; therefore, one can estimate the respective time delays $t31$ and $t32$, with which the angle θ of the propagating front with geographic axis north–south and front speed V can be computed:

$$\tan\theta = t31/t32 \quad (8)$$

and

$$t31 = d/V\cos\theta, \quad t32 = d/V\cos(\pi/2 - \theta). \quad (9)$$

These parameters have been estimated from the covariance function of reflectivity between antennas at different levels, following the method of Eymard and Weill (1979). As the repetition period has been improved (4 s now instead of 8) and as the angle between antennas 1 and 2 is now 90° instead of 120°, the precision of measurement is found to be

$$\Delta V/V \approx \Delta t_{ij}/t_{ij} \approx d\theta/\theta \approx 0.15,$$

where tij is the time delay between antennas i and j. Hence, wind components parallel to the front in the region 1 and 2 are computed with the geometry of Fig. 3, in which Ψ is the angle between horizontal wind velocity $\mathbf{U}(U, \Psi)$ and geographic axes, θ' the angle between $\mathbf{V}(V, \theta')$ and the same axes, α the angle between wind velocity and x axis and β the angle between $\mathbf{U}$ and $\mathbf{V}$. These different components are computed for region 1 and 2 and are indexed accordingly (Fig. 3c).

The foregoing analysis of the Doppler sodar information used to yield the frontal velocity vector and the wind components along the frontal axis can be used to study the frontal slope, the slope modifications due to divergence of vertical momentum transfer, [Eq. (3)] and also to estimate the frontal drag coefficient from Eq. (6).

4. Case study

Based on the previous methodology, various cases of fronts observed during the Mesogers 84 experiment have been analyzed in conjunction with surface measurements of the meteorological parameters at Patac stations.

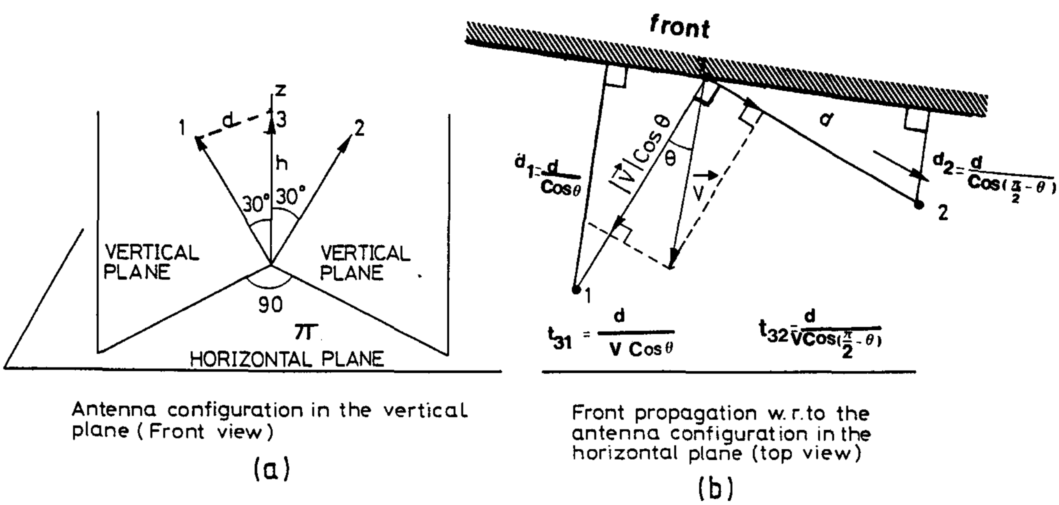

FIG. 2. (a) Sodar antennas configuration: antenna 3 is vertical. (b) Representation of delays $t31$ and $t32$ observed between antennas 3, 1 and 3, 2 when the frontal surface is passing over antennas: ($t31 + t12 + t23 = 0$).

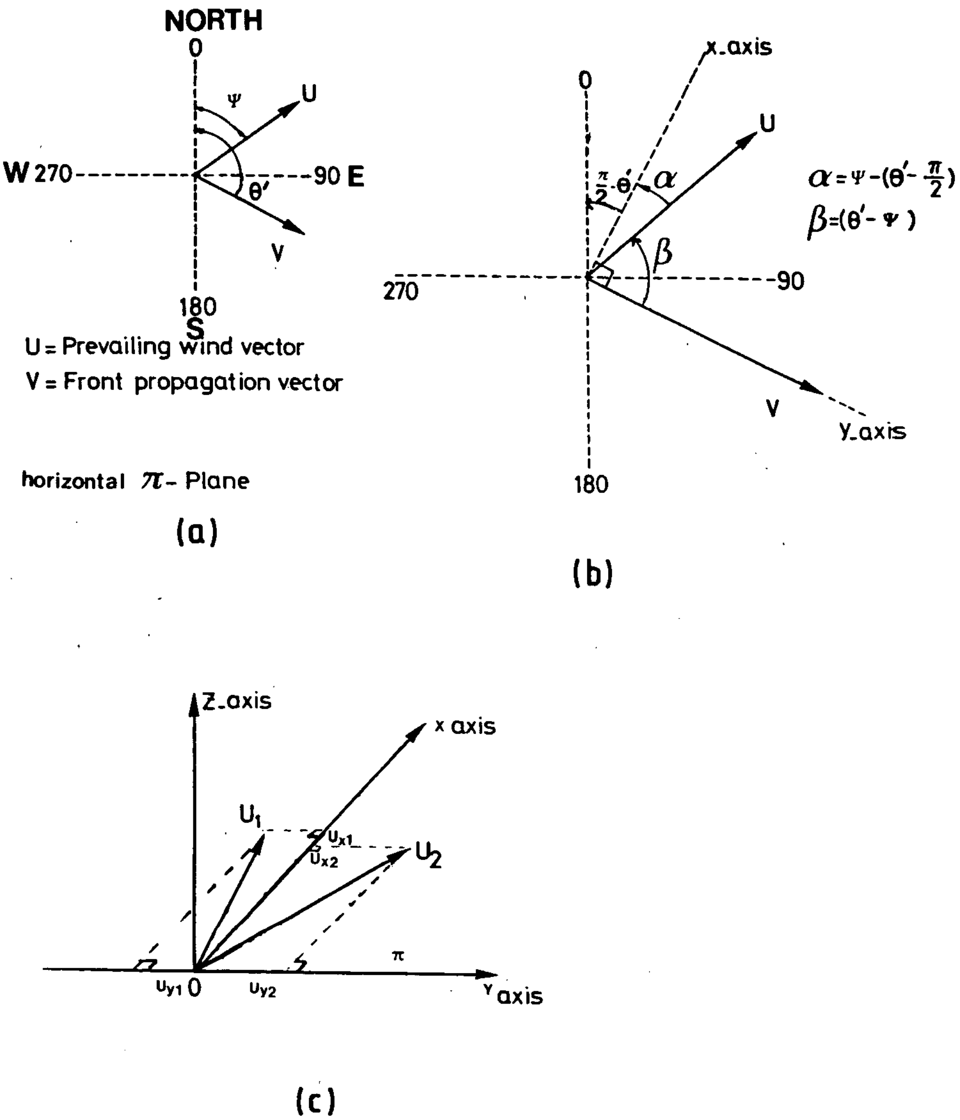

FIG. 3. (a) Representation of horizontal wind vector **U** and frontal propagation velocity **V** with respect to geographic axes (0 for north, 90 for east, 180 for south, 270 for west). (b) As in 3a but with respect to frontal axes. (c) Geometry of horizontal wind components before and after the frontal interface with respect to frontal coordinates.

To illustrate the use of the various equations, a case study for the frontal system observed on 13 September is presented. The frontal echograms from sodars 1, 2 and 3 are shown in Fig. 4a. The time delays $t31$ and $t32$ (here in the lower part of the facsimile records), with respect to the reference point A, are 62 s and 31 s, respectively. The angle θ (formula 8) is close to 63° ± 9°, with a propagation velocity of 6.2 ± 0.9 m s^{-1}. Using the geometry of Fig. 3 we get $\theta' = 103° \pm 9°$. The wind field at 1958 UTC, representative of region 1, is $U_1 = 2.4 \pm 0.3$ m s^{-1} and $Y_1 = 127° \pm 10°$, and at 2039 UTC is $U_2 = 4.8 \pm 0.3$ m s^{-1}, $Y_2 = 303° \pm 10°$: the incertitude on Y_1 and Y_2 correspond to wind azimuth sodar estimate $\approx 10°$.

Taking the components along the x-axis, we obtain $u_{1x} = 1 \pm 0.2$ m s^{-1} and $u_{2x} = 1.6 \pm 0.3$ m s^{-1} (the incertitude of 20% takes into account incertitude of α and U). With a temperature difference $|T_1 - T_2| = 0.5 \pm 0.1$°C, the classical slope is close to 0.2° while the sodar-derived real slope is 5.2°, which means the slope modification due to frontal friction is 5.0°, 20 times larger than the classical slope by itself.

Estimation of the drag coefficient requires the velocity components in the horizontal direction of front propagation. These can be computed through wind components along y (u_{y1} and u_{y2}). The computed wind profiles along the y axis for the periods as before (1958 UTC) and after (2030 UTC) are shown in Fig. 4b, to-

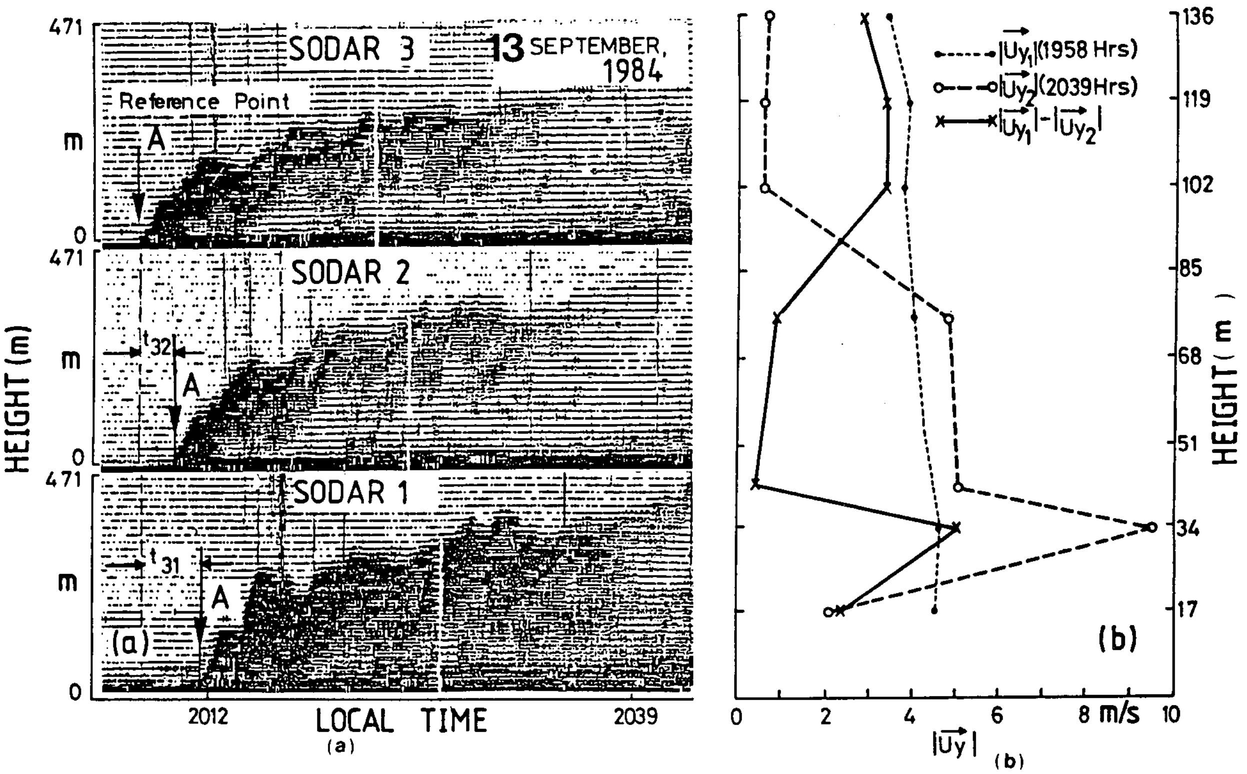

FIG. 4. (a) Numerical facsimile record of reflectivity (echograms) showing observed time delays from a frontal system passing over the three antennas of the sodar system, on 13 September, during Mesogers 84 experiment. Numerical facsimile records here mean that reflectivity is computed from Doppler spectra and hence, corresponds to numerical data as opposed to the analogical facsimile records generally used. (b) Vertical profiles of mean horizontal wind components parallel to the frontal motion before and after the front interface, and vertical profiles of the differences.

gether with the computed wind profile difference $|u_{y1} - u_{y2}|$. This gives a wind-gradient difference term $\partial/\partial z\,(\Delta u_y)^2$ close to 1.3 in the surface layer. Taking the divergence of momentum transfer $\partial/\partial z\,(\tau_1 - \tau_2)$ to be 1.5×10^{-3} corresponding to the slope modification of 5°, the frontal drag coefficient C_{df} becomes $(3.1 \pm 2.1) \times 10^{-3}$; an incertitude of 70% on C_{df} corresponds to an incertitude of 30% on the friction term of Eq. 3,

TABLE 1. Results of the analysis of front propagation velocity, front slope, drag coefficient, and front type (characterized with or without precipitation).

			Front slope					
Date (1984)	Time (LST)	Front propagation velocity (m s^{-1})	(1) from SODAR (deg)	(2) classic from temperature and wind field (deg)	(1–2) difference (deg)	Drag coefficient C_{df}	Nature of the front*	Followed by precipitation?
11 Sep	2128	9.0 ± 1.4	1.6 ± 0.2	0.2 ± 0.03	1.4 ± 0.2	$5.1 \pm 3.6 \times 10^{-1}$	+	No
13 Sep	2012	6.2 ± 0.9	5.2 ± 0.8	0.2 ± 0.03	5. ± 0.8	$3.1 \pm 2.2 \times 10^{-3}$	+	No
26 Sep	0413	8.2 ± 1.2	2.5 ± 0.4	0.3 ± 0.05	2.2 ± 0.5	$6.5 \pm 4.6 \times 10^{-2}$	−	No
28 Sep	1857	2.6 ± 0.4	17. ± 3.	1. ± 0.2	16. ± 3.	$8.2 \pm 5.7 \times 10^{-3}$	+	Yes
29 Sep	1917	1.9 ± 0.3	11. ± 2.	0.2 ± 0.03	10.8 ± 2.	$2.9 \pm 0.2 \times 10^{-3}$	−	Yes
29 Sep	1711	6 ± 0.9	2.2 ± 0.3	0.1 ± 0.03	2.0 ± 0.3	$9.4 \pm 6.6 \times 10^{-2}$	−	Yes
4 Oct	1345	6. ± 0.9	2.1 ± 0.3	0.1 ± 0.02	1.9 ± 0.3	$3.0 \pm 2.1 \times 10^{-2}$	−	Yes
5 Oct	0318	6. ± 0.9	4.1 ± 0.6	0.1 ± 0.02	4.0 ± 0.6	$6.3 \pm 4.4 \times 10^{-2}$	−	Yes
10 Oct	0434	5. ± 0.8	1.4 ± 0.2	1.1 ± 0.2	0.3 ± 0.4	$1.6 \pm 1.1 \times 10^{-2}$	−	Yes

* Cold −/warm +.

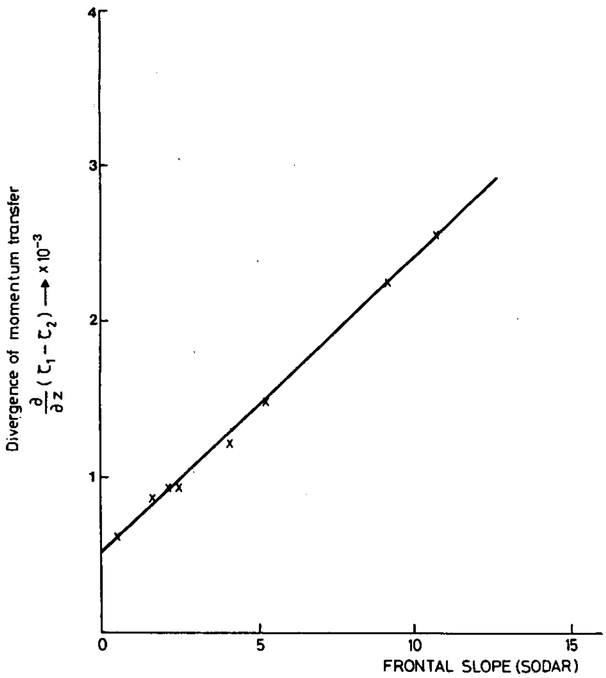

FIG. 5. Divergence of momentum transfer estimate related to frontal motion as a function of observed frontal slope during the Mesogers 84 experiment.

and an incertitude of $\approx$40% on $\partial/\partial z(\Delta u_y)^2$. The values $g = 9.8$ m s^{-2}, $f = 1 \times 2\ 10^{-4}$, $\rho = 1.3$ kg m^{-3} are used.

5. Results

Results of the analysis of nine frontal cases observed during the experiment are listed in Table 1. It is seen that the friction contribution to the Doppler-derived front slope is considerable and dominates the classic frontal slope. Frontal slope is found to be proportional to the divergence of the momentum transfer (Fig. 5) associated with the friction velocity in the surface layer, and does not seem to have any systematic dependence on the front propagation velocity.

A study of the variation of the frontal drag coefficient with the propagation velocity shows (in Fig. 6) that with or without precipitation the drag coefficient tends to increase with propagation velocity, which could imply that $\partial/\partial z(\Delta u_y)^2$ must decrease when V increases. However, more data are necessary to draw any significant conclusion from this. Estimated drag coefficient values are quite realistic, lying close to, but generally higher than, the typical geostrophic drag coefficient value $\approx 2 \times 10^{-3}$ (Smith, 1975).

A study of the relation between updraft and downdraft velocities (averaged for each set of five altitude gates) and the horizontal wind speed at the top of the surface layer has been made at five representative levels (Fig. 7) using the hypothesis that horizontal wind velocity U is proportional to U_*. It is observed that with increasing wind speed, the downdraft velocity increases at all levels. This suggests that the fronts associated with the largest downdrafts are observed under the highest horizontal wind velocity, showing that friction velocity in the wind direction joined to the friction velocity in the direction of frontal movement is an important parameter to be known. Figure 7 presents mainly downdraft motions which statistically correspond to the characteristics of occurred frontal systems; updraft motions exist systematically during short time periods in "gust fronts" just before fronts, however, and as only nine cases of fronts are observed here, updraft motion is thus statistically not very well represented.

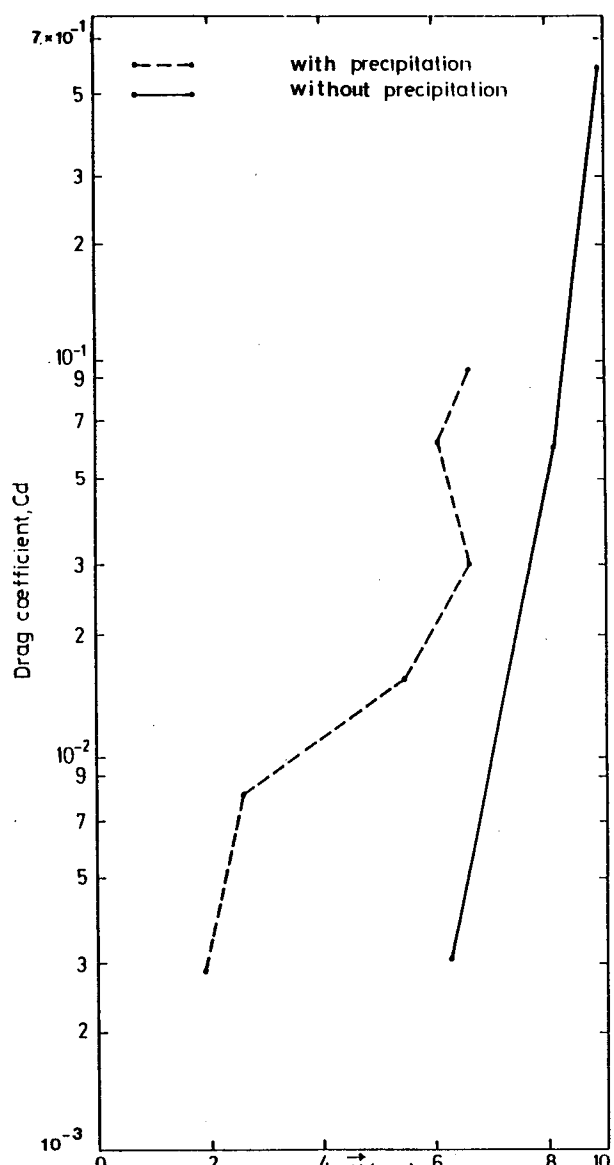

FIG. 6. Drag coefficients as a function of front velocity (continuous line, front associated with precipitation; dotted line, front without precipitation).

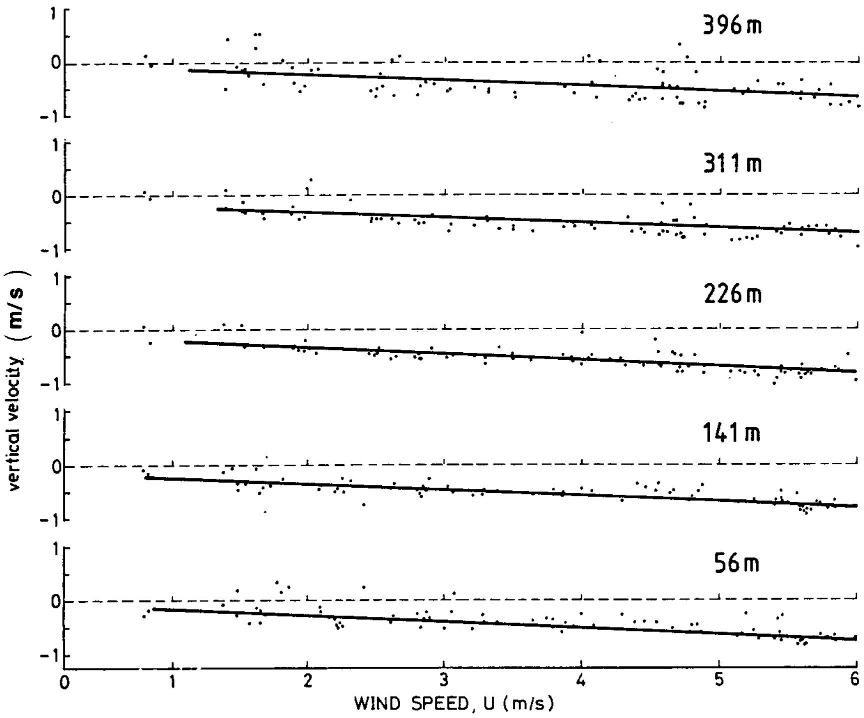

FIG. 7. Vertical velocity averaged along 20 min and on five gates as a function of horizontal wind speed measured at 20 m height during Mesogers 84 experiment.

6. Conclusions

Using Doppler sodar, a method has been derived to compute frontal slopes and friction-induced vertical momentum transfer. Results show that divergence of momentum transfer considerably modifies the frontal slope to an extent that must be considered in parameterization of the planetary boundary layer; this result shows the importance of correctly estimating the frontal friction in numerical modeling. It has to be noted that in a homogeneous boundary layer only Reynolds stress parallel to surface-layer shear is the relevent parameter. In the presence of mesoscale systems such as fronts, a systematic knowledge of stress components along mean wind direction and parallel to frontal motion is necessary.

This study—presenting a limited number of cases, and only considering mean frontal slopes in the lower part of the boundary layer—has to be further pursued looking not at the mean slope but to the slope variation as a function of height. Our sodar methodology seems to be an interesting tool for this goal but we have to add other measurements: S.T. radars for obtaining wind profiles in the "free atmosphere" with a matching part with Doppler sodar in boundary layer, momentum flux measurements in the surface layer made with appropriate instruments in such a way as to obtain redundant measurements of friction; this would help to obtain more definitive results and could improve C_{df} incertitude.

Acknowledgments. The authors would like to thank very much their colleagues who participated in the Mesogers 84 experiment and colleagues from SMIRSO (Bordeaux Mérignac) for providing Patac meteorological data. Special thanks are due to C. Mazaudier for her technical and computational assistance. This study has received financial support from INSU (Contracts 4647 and 4687), and by CNET. The authors would also like to very much thank their referees for very useful and constructive comments.

REFERENCES

Eymard, L., and A. Weill, 1979: A study of gravity waves in the planetary boundary layer by acoustic sounding. *Bound.-Layer Meteor.*, **17**, 231–245.

Johnson, R. H., and M. E. Nicholls, 1983: A composite analysis of the boundary layer accompanying a tropical squall line. *Mon. Wea. Rev.*, **111**, 308–319.

Long, R. R. and W. Shaffer, 1975: Some physical and numerical aspects of the boundary layer modelling. NOAA Tech. Mem. NWS-TDL-56.

Mason, P. J., and R. I. Sykes, 1978: On the interaction of topography and Ekman boundary layer pumping in a stratified atmosphere. *Quart. J. Roy. Meteor. Soc.*, **104**, 475–490.

Scott, R. W., and B. Ackerman, 1983: Surface signatures of a dry nocturnal gust front. *Mon. Wea. Rev.*, **111**, 197–204.

Smith, F. B., 1975: Turbulence in the atmospheric boundary layer. *Sci. Proc. Oxford*, **62**, 127–151.

Weill, A., T. Baudin, J. P. Goutoree, P. Van Grunderbeeck and P. Le Berre, 1978: Turbulence structure in temperature inversion and in convection fields as observed by Doppler sodar. *Bound.-Layer Meteor.*, **15**, 375–390.

——, C. Mazaudier, F. Baudin, C. Klapisz, F. Leca, M. Masmoudi, D. Vidal Madjar, R. Bernard, O. Taconet, B. S. Gera, A. Sauvaget, A. Druilhet, P. Durand, G. Dubosclard, J. Y. Caneil, P. Mery, A. G. M. Beljaars, W. A. A. Monna, J. G. Van Der Vliet, M. Crochet, D. Thomson and T. Carlson, 1986: *MESOGERS 84 Experiment*, 33 pp, submitted.